High-voltage control of an electrostatic precipitator by automatic motorized potentiometer (amp). In-situ measurement of the surface potential of the pollution layer

Haskar Houari, Miloua Farid, Oualid Imene, Ouari Abbes, Tilmatine Amar
Dept. of electrical Engineering
APELEC Laboratory, Djillali Libes University, Sidi Bel Abbes, Algeria
phone: (213) 560-713-783
e-mail: houssemeddine_h@yahoo.fr
e-mail: milouafarid@gmail.com

***Abstract*—Electrostatic precipitators (ESPs) are the most common devices used to separate dust, fumes or fog from a gas. Many factors are involved in the filtration process, which requires optimization and continuous monitoring of collection efficiency. The resistivity is one of the important factors that significantly affects the performance of an ESP. It has a particular effect on the behavior of the dust layer once deposited on the collecting electrode. The particles (e.g. PVC) that exhibit a high resistivity are difficult to charge, but once charged, they do not easily give up their acquired charge in contact with the ground electrode, which causes an increase in surface potential and consequence the appearance of back corona phenomenon. Therefore, in order to have an optimal filtration efficiency, the electric field intensity must be as high as possible (close to the breaking voltage) in order to ensure a better loading of the particles which have high resistivity, but without provocation an electric arc. The purpose of this article is to propose a new practical technique for the control of a wire-cylinder configuration ESP, based on the automatic variation of the high voltage by a motorized potentiometer (PM) in order to maintain the set point discharge current. Automatic voltage control varies the power of the high voltage power supply in response to signals received from the ESP. The surface potential of the pollution layer as well as its resistance can be deduced in-situ under electrical discharge for different particle sizes. The estimation of the thickness of the dust layer (as a function of time) is possible since the density of the dust is known.**

I. INTRODUCTION

Electrostatic precipitation is a way used to eliminate solid pollutants (such as dust and ashes) or liquids (oil mist for example) contained in the gas injected into our environment. No other filtering process is as effective as the electrostatic process, its scope extends currently to viable places (apartments, offices, hospitals, etc ...) as well as workshops (machine rooms) given its low electrical energy consumption and its high filtration efficiency (up to 99.9%) [1]. Nevertheless, and despite this efficiency high, the ESPs are always affected by physical parameters (related to the gas and dust) which have a great influence on their performance [2-3].

The resistivity of the dust layers collected on the electrode is a very important feature to control the performance of a precipitator [4-5]. It is a parameter related to the physico-chemical nature of the dust. A High resistivity will cause back-discharge [6-7], which creates an arc between the two electrodes. This change in discharge regime (from the diffuse corona discharge regime to the arc regime) significantly reduces the efficiency of the collection [8].The resistivity of the particles or a porous layer of particles is therefore an important parameter for the choice of the operating voltage and the reference current. A resistivity between 10^{+2} and 5.10^{+8} Ω.cm allows a normal functioning of the ESP [9]. We chose PVC particles with known resistivity (greater than 10^{+8} ohm.cm), which allows to have an abnormal functioning of the filter, so it makes extensive use of an online control and command system. The command adopted in this paper is an automatic voltage control by ARDUINO card, which allows varying the power supply voltage, so that the sparks in the ESP are extinguished on a timely basis [10-11]. In addition to the control system, the aim of this work is to study the experimental feasibility of a resistance measure system of PVC powder layer accumulated over time on the surface of the collector electrode of the ESP [12-13]. The deduction of this resistance as well as its surface potential is possible by an In-Situ measurement of the discharge current, which must be fixed according to the selected set-point [14].

II. MATERIALS AND METHODS

A. Experimental device

The test bench realized (Fig.1), can be divided into three separate functional entities: the admission part of the PVC powder, the filtration device and the part of command and control of the ESP. The admission of the PVC powder (majority size of 180-µm diameter) is provided by a vibro-transporter which introduces it directly into a funnel placed at the entrance of the ESP for a fixed mass flow q_{int} = 0.5 g/s. The speed of the powdery flow is controlled by a dust recovery cyclone (Q_{max} = 150 m^3 / h) which allows to recover the unfiltered powder. The filtration device is a conventional ESP wire-cylinder in horizontal position 140 mm long and 90 mm in diameter. The corona wire of diameter 0.25 mm is connected to a negative high voltage supply (U_{max} = 40 kV, I_{max} = 7.5 mA, Model SL-300, Spellman). The control part of the filter consists mainly of an ARDUINO MEGA card, a motorized potentiometer and voltage sensors.

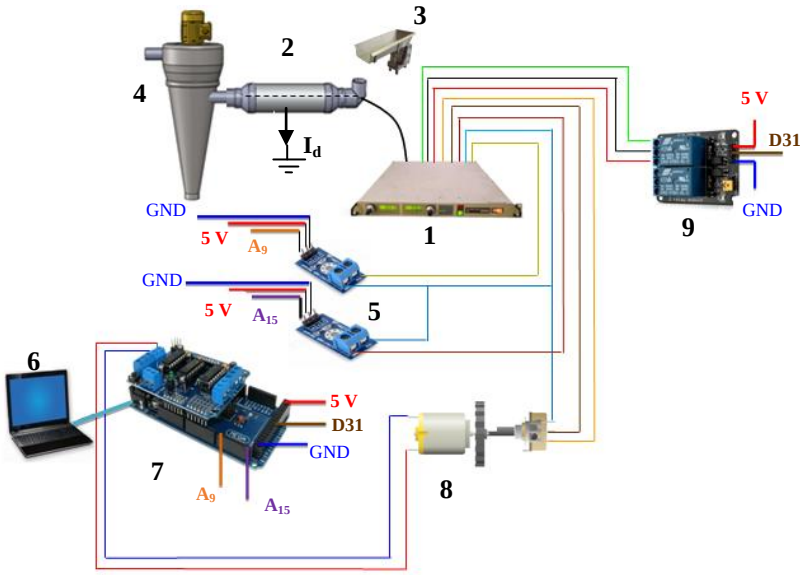

Fig. 1.Circuit of the autopilot of the high-voltage power supply (Machine-Machine Interface):1. Spellman high voltage power, 2.ESP, 3.Vibro-transporter, 4.Recovery cyclone, 5.Voltage sensors, 6.Computer, 7.Arduino + Shield motor, 8. Motorized potentiometer, 9.Relay module.

A. Procedure of the control technique

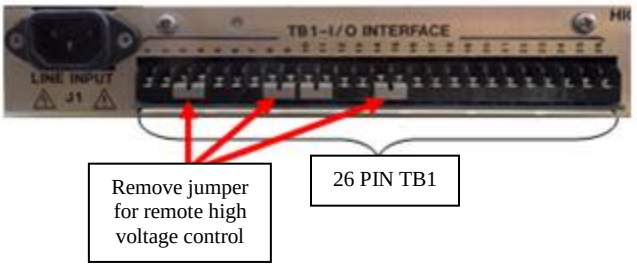

Fig. 2.External interface of the HT generator (the rear of the chassis).

The HT Generator (SPELLMAN SL-300) used [15], incorporates several features that allow a progressive manual increase in the high voltage until the predefined operating point. In local control (front panel control) of the power supply, jumpers are installed on the external interface TB1 (or J5) in the rear of the chassis between TB1-10 (J5-10) and TB1-11 (J5-11) for voltage control and between TB1-8 (J5-8) and TB1-9 (J5-9) for current control (Fig. 2). For an automatic control, the jumpers are removed and a positive voltage source is applied to the appropriate terminals. By adjusting the voltage source of the low power circuit from 0 to 10 V, a voltage change is obtained at the high power circuit (0 kV to 40 kV). Pins 5 and 6 on the back panel are used to monitor the current and output voltage (Fig. 3).

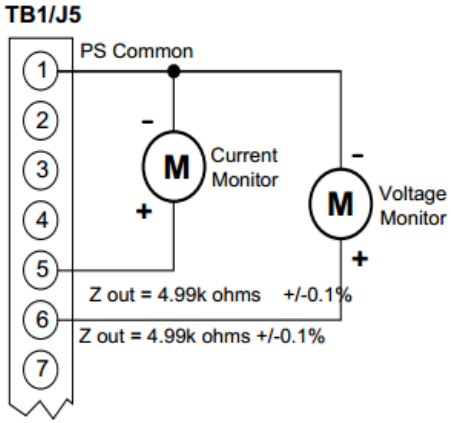

Fig. 3.Circuit for sampling the current and the voltage delivered by the high voltage generator.

The circuit diagram is shown in Fig.4. We observe that 4 distinct elements are connected to the Arduino card:

- Two voltage sensors, allowing data transfer (voltage and current);
- A relay module that opens or closes the power switch (ON and OFF) and in the case of an arc disables automatically the high voltage power supply;
- A motorized potentiometer for the automatic adjustment of the voltage of the low power circuit of the power supply;
- A shield module for the control of the potentiometer motor that generates a pulse width modulation (PWM) signal.

The Arduino (the central element) periodically collects the measurements taken by the voltage sensors. The discharge current delivered by the ESP is continuously compared with the set-point current. If exceeded, the Arduino card automatically reduces the supply voltage of the source via the motor shield in order to increase the resistance of the potentiometer.

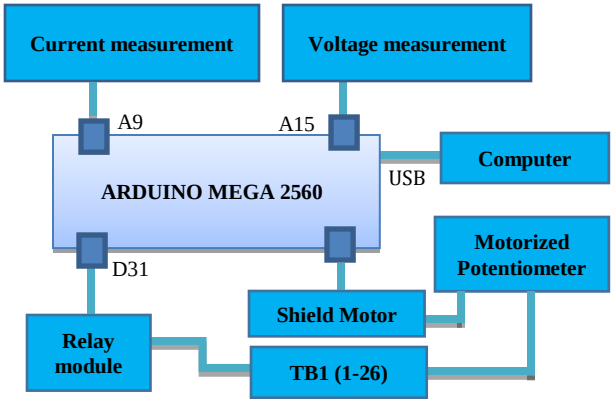

Fig. 4.Illustrative diagram of the control circuit.

B. Determination of the set-point current ($I_{set\text{-}point}$)

Before start-up the ESP with its automatic control system, you must first determine the limit of its normal operation; this is accomplished by varying the voltage manually at the highest level without causing spark excess between the two electrodes. In practice, a better filtration is obtained when the applied voltage is close to the breakdown voltage, especially when the particles to be filtered have a high resistivity such as PVC. From Figure 5, the set-point current must not exceed 1.4 mA.

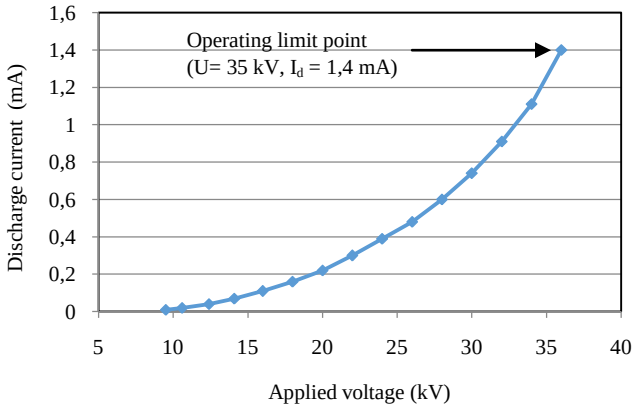

Fig. 5.Determination of the operating limit point of the precipitator.

C. Command protocol

After manual determination of the set-point current, we are moving now to the programming of the ESP control voltage. The Serial communications provide a simple and flexible way to communicate the Arduino MEGA with the computer. By connecting the serial port of the Arduino to the computer, we can easily load the sketch (program). This process sends data from the computer to the Arduino, and the Arduino in turn sends status messages to the computer to confirm that the transfer is successful. The commands sent from the Arduino card via the shield motor allow the motorized potentiometer to rotate in both directions at the required speed for a $t_{forward}$ or $t_{backward}$, in order to regulate the high voltage to maintain a fixed discharge current. This last is continuously compared on a sampling step ($t_{measure}$) with the consigned current. A block diagram of principle outlining describing the control protocol functionality is shown in Fig 6.

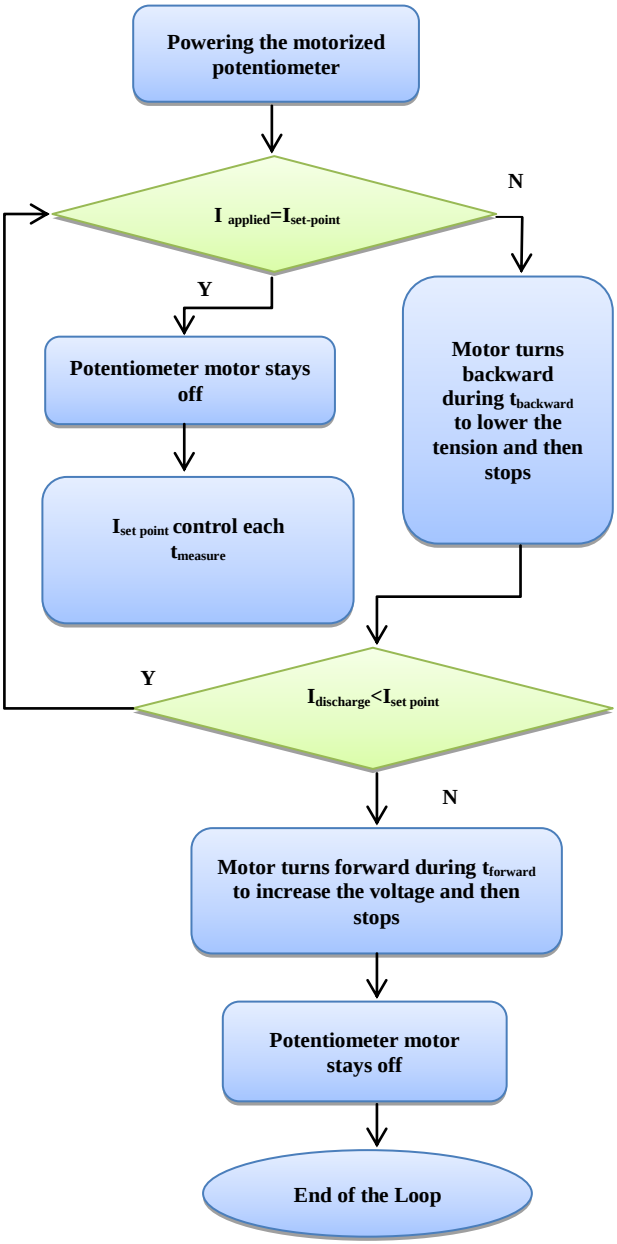

Fig. 6. Block diagram of the voltage control and its operation.

III. EXPERIMENTAL RESULTS AND DISCUSSION

The automatic voltage control technique allows us to record the analog value of the discharge current and the voltage applied using the function ana1ogueRead (). Note that the potentiometer delivers an analog voltage between 0V (TB1-1) and 10V (maximum value of TB1-7). The servo control in voltage must be done numerically by comparing between the applied current value and the set-point current value in order that the shield motor can generate appropriate PWM signals, which powers the motorized potentiometer. The generation of PWM must respect the response time of the control system. For this reason, the rotation time of the potentiometer $t_{forward}$ and $t_{backward}$ must be mastered by the Arduino program, in order to limit to the maximum the frequency of sparks.

III. 1 PERFORMANCE ANALYSIS OF ESP

A. Efficiency of filtration with or without the voltage control

According to the results shown by the figure 7 and by analyzing the results of table 1, we note:

- An increase, almost double the filtration efficiency for different operating times of the filter.
- Significant reduction in the number of sparks.

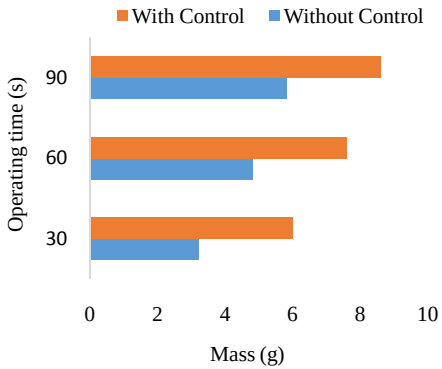

Fig. 7.Comparison of the ESP performance without and with automatic control.

Table 1: Comparative results of the filtration efficiency.

experiments	Time (s)	collected mass (g)	Number of sparks	Efficiency (%)
without control	30	3,2	20	21,33
	60	4,8	>20	16
	90	5,8	>30	12,89
Automatic control	30	6	1	40
	60	7,6	1	25,33
	90	8,6	1	19,11

Figure.8 illustrates the on-line variation of the discharge current following triggering of the automatic high voltage control, for an operating time of the ESP equal to 210s. It is quite clear that the response of the control system is almost instantaneous since the nominal operating regime is reached. The current stabilizes around the set-point current equal to 0.9mA, after passing through an unstable operating regime (very frequent presence of sparks).

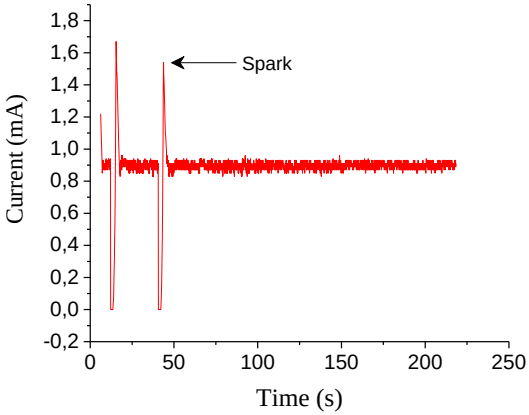

Fig. 8.Online variation of the discharge current.

Furthermore, during filtering, the collected dust layer begins to behave as an ascending variable resistance, thereby increasing its surface potential [16]. Fig. 9 represents the surface potential measured experimentally in real time. There for, and in order to keep a fixed discharge current in the neighborhood of the set-point current ($I_{set\text{-}point}$ = 0.9mA), the regulation system decreases the applied voltage (Figure 11) as the PVC particles settle on the collection electrode. The recorded voltage drop is proportional to the resistance of the PVC layer since the discharge current is maintained constant. It can be calculated by the following relationship:

$$U_{App} - U_{Ins} = V_{Sur} = R_{PVC}(t).I_{set-point} \quad (1)$$

With:
U_{App} : Applied voltage (35 kV);
U_{Ins} : Instantaneous voltage applied (kV);
V_{Sur} : Surface potential (kV);
$R_{PVC}(t)$: Resistance of the PVC layer as a function of time;
$I_{set-point}$: Fixed set point current (0.9 mA).

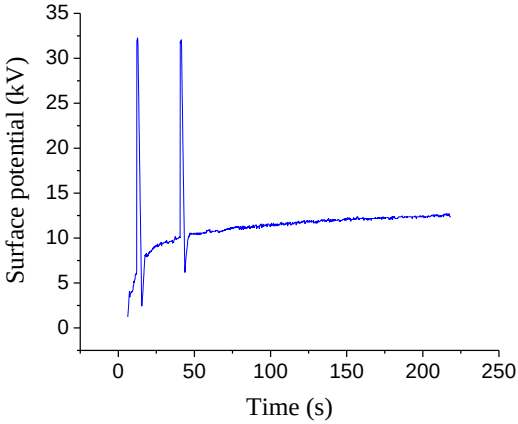

Fig. 9.Temporal variation of the surface potential of the PVC layer.

B. Influence of particle size on surface potential

The dust deposited on the collection electrode behaves as a variable resistor in series with the ESP. According to the figure 10, it is clear that the surface potential is increasing regardless of the size of the particle. This is due to the increase in the amount of material collected as a function of time which leads to the increase of its resistance. The latter is inversely proportional to the particle size (Table 2). Indeed, as the size decreases, the inter-particle distance also decreases, which considerably reduces the dissipation of electric charges to the ground. Note also that despite the mass collected for a size of 90 µmm is smaller compared to a size of 125 µm and 180 µm, the value of the recorded resistance is significantly higher.

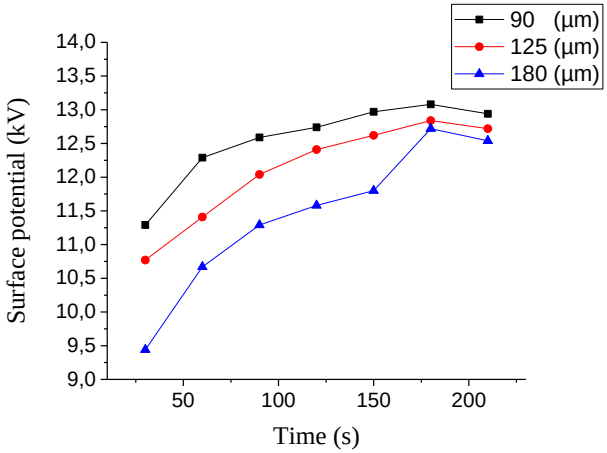

Fig. 10.Variation of the surface potential according to the size of the PVC particles.

TABLE 2: RELATION BETWEEN THE MASS AND RESISTANCE OF THE COLLECTED DUST LAYER.

Particles diameter (µm)	90		125		180	
Operating time (s)	M_c(g)	R (MΩ)	M_c(g)	R (MΩ)	M_c(g)	R (MΩ)
30	3	12,66	4,1	12,016	6	10,57
60	4,4	13,5	5,5	12,75	7,6	11,88
90	5,3	14	6,5	13,54	8,6	12,62
120	6	14,45	7,3	14	9	12,95
150	6,6	14,8	7,7	14,2	9,6	13,45
180	7	15	8,2	14,54	10,3	14,19
210	6,2	14,67	7,5	14,29	10,1	14

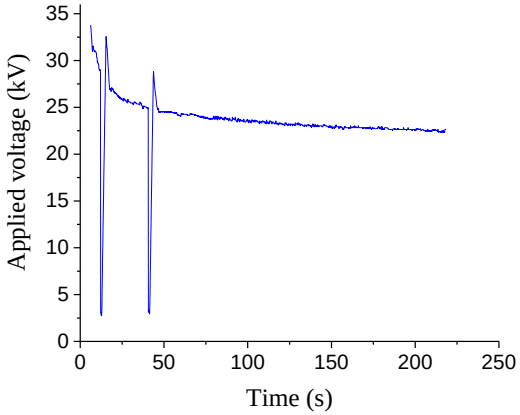

Fig. 11.Online regulation of the applied voltage.

C. Relationship between the resistance and mass of the collected PVC layer

In order to find a relationship between the resistance and the mass of the collected PVC powder, mass measurements have been performed for different operating times of the ESP (Figure 12). We note that the collected mass reaches its maximum value for a time of 180 s, this is due on the one hand to the saturation of the collection electrode and on the other hand to the excessive increase of the voltage drop.

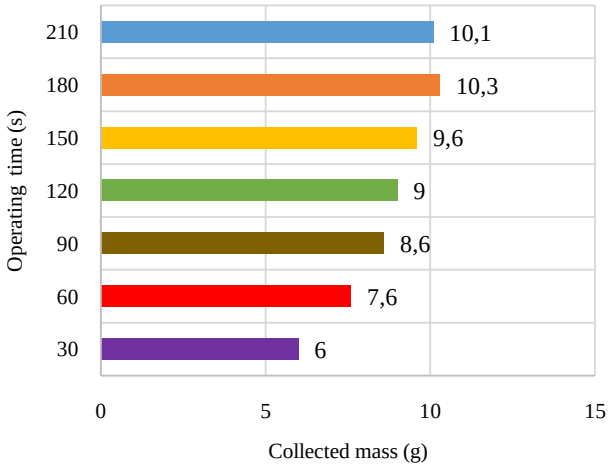

Fig. 12.Variation of the collected mass as a function of time.

From the Relationship (1) we can calculate the resistance value of the PVC layer, its given by:

$$R_{PVC}(t) = \frac{U_{App} - U_{Ins}}{I_{set-point}} \qquad (2)$$

Table 3: Numerical values of the mass and resistance of the PVC layer.

Operating time (s)	**M_{PVC} (g)**	**R_{PVC} (MΩ)**
30	6	10,57
60	7,6	11,88
90	8,6	12,62
120	9	12,95
150	9,6	13,45
180	10,3	14,19
210	10,1	14

Plotting now on the same figure (Fig.13) the variation of the mass as well as the resistance of the PVC layer as a function of the operating time of ESP. It is clear that the two variations follow a same pace, so we can say that the resistance increases as a function of the mass of dust collected. This variation is quasi-linear (fig.14).

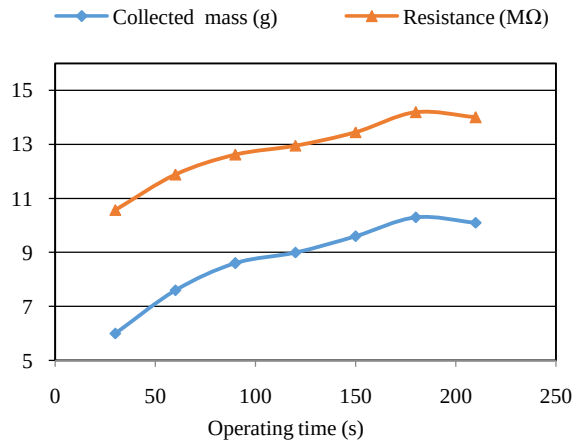

Fig. 13.Evolution of the resistance and the collected mass of PVC as a function of time.

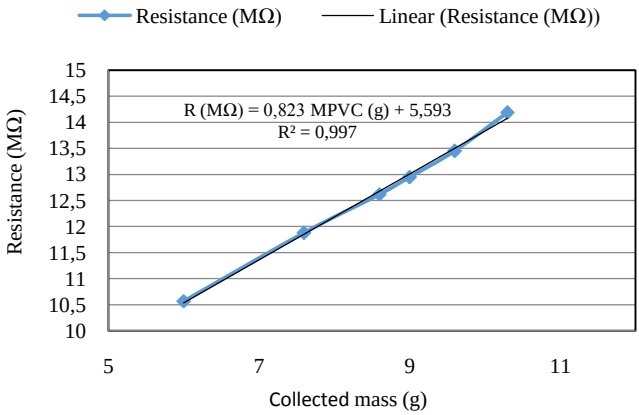

Fig. 14.Variation of the PVC layer resistance as a function of the collected mass.

III. 2 MODELING OF THE FILTRATION PROCESS

A. Online Prediction of Filtration Efficiency

In order to predict the performance of the filter as a function of time, we must know either the collected mass or the outgoing mass. Since there is linearity between the resistance and the collected mass, then we can express the efficiency as a function of the resistance of the PVC layer. According the prediction curve of Figure 15, the efficiency can be put in the following form:

$$\mu(t) = \frac{M_{pvc}(R)}{t.q_{int}}.100 \qquad (3)$$

Or:

$$\mu(t) = \frac{(1{,}21\,.R_{PVC}(t) - 6{,}743)}{t.q_{int}} \qquad (4)$$

With:

$M_{pvc}(R)$: Mass collected as a function of the resistance of the layer (g);

q_{int} : Mass flow of particles of PVC introduced in the ESP (0,5g/s);

$R_{PVC}(t)$ Resistance of the PVC layer (equation 2);

t: Filter operating time (s).

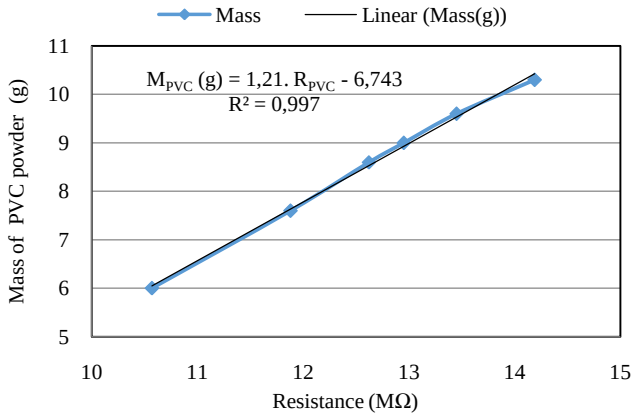

Fig. 15.Plot of the variation of the mass collected as a function of the measured resistance.

The efficiency variation as a function of time according to the relationship (4) is represented by the following figure:

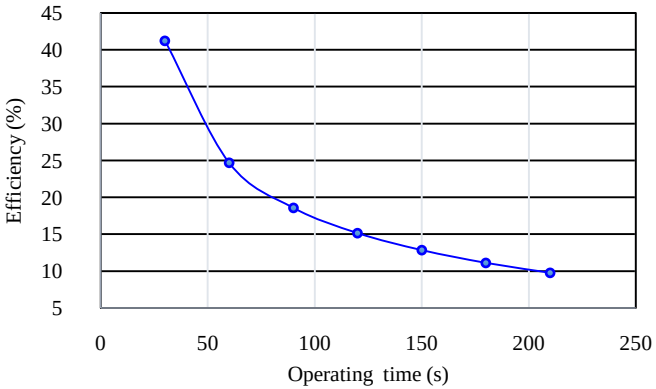

Fig. 16.Online variation of filtration efficiency.

We find that the efficiency is maximum when the resistance value of the collected layer is maximum. For our experimental conditions, the rapping cycle must be less than 60s in order to ensure a yield close to 40%, which corresponds to a R_{PVC} resistance of less than 11.88 MΩ.

B. In-situ measurement of the resistivity of the PVC layer

The in-situ principle consists in measuring the resistivity of a material during an electric discharge. The difficulty is to precisely determine the surface potential $VSur$ to which there is the material. According to this method the resistivity can be expressed by:

$$\rho_{PVC} = \frac{V_{Sur}}{e.J} \qquad (5)$$

where 'ρ_{PVC}' is the electrical resistivity, 'e' is the thickness of the dust layer and 'J' is the density of the surface current.

There is another relationship for determining the resistivity of a dust layer. It is obtained from the standard IEEE method which consists in depositing a layer of dust in a cell placed between two parallel electrodes, then a voltage of a few kilovolts is applied on the electrode system. The resistivity is thus calculated by measuring the current flowing through the dust layer. This relationship is given by:

$$\rho_{PVC} = \frac{S.U_{Ins}}{I_d.d} \qquad (6)$$

With 'S' is the surface of the cylindrical shaped collection electrode, 'd' is the inter-electrode distance and 'I_d' is the instantaneous discharge current.

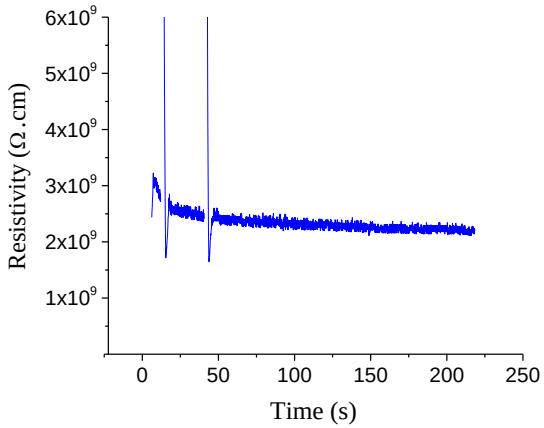

Fig. 17.Online measurement of the resistivity of the PVC layer.

The figure.17 shows an online sampling of the resistivity, each $t_{measure}$ for duration of 210s calculated from relationship (6). The average value of the resistivity is approximately $1.5.10^{+9}$ Ω.cm. It is for this reason that the frequency of sparks is very frequent without the use of a voltage control system.

IV. Conclusion

This study was initially focused on controlling the voltage of an ESP by a motorized potentiometer. In effect, this technique is very practical and has considerably reduced the frequency of sparks, through an automatic control of the discharge current produced by the ESP, which allows an increase in the collection efficiency to almost the double of its value. The In-situ measurement of the resistivity of the dust layer as a function of time is possible when the value of the surface potential is well measurable. The resistivity of a dust deposit depends on many factors such as particle size, compactness of the deposit, applied electric field strength, temperature and humidity. On the other hand, the instantaneous measurement of the resistance of the pollution layer leads to an online evaluation of the efficiency of the filtration.

REFERENCES

[1] S. Oglesby, G.B. Nichols, “Electrostatic Precipitation, “Marcel Dekker Inc, New York, 1978. M. Akay, Time Frequency and Wavelets in Biomedical Signal Processing (Book style). Piscataway, NJ: IEEE Press, 1998, pp. 123–135

[2] T. Yamamoto, H. R. Velkoff, "Electrodynamics in an electrostatic precipitator, "J. Fluid Mech., vol. 108, pp. 1-18, 1981.V. Medina, R. Valdes, J. Azpiroz, and E. Sacristan, “Title of paper if known,” unpublished.

[3] J. Podliski, A. Niewulis, J. Mizeraczyk, P. Atten, "ESP performance for various dust densities", J. Electrostat., vol. 66, no. 5/6, pp. 246-253, May 2008.

[4] Busby, H. G. Trevor, and K. Darby, “Efficiency of electrostatic precipitators as affected by the properties and combustion of coal,“J. Inst. Fuel 36, no. 5, pp.97-184, 1963.

[5] J. Miller, B. Hoferer, A. J. Schwab, “The Impact of Corona Electrode Precipitator Performance“, J. Journal of Electrostatics, vol. 44, pp. 67-75,1998.

[6] S. Masuda, and A. Mizuno, “Flashover measurement of back discharge, “J. lectrostatics, Vol. 4, pp. 215, 1978.

[7] C. Chesmond, R.J. Truce, “Using Electrostatic Precipitators to Collect Highly Resistive Dust,” Institute of Engineers Australia, Queensland Technical Papers. Vol. 26, no.9, pp 16- 20, June 1985.

[8] White, J. Harry, “Resistivity problems in electrostatic precipitation, " Journal of the Air Pollution Control Association, vol. 24, no. 4, pp. 313-338, 1974.

[9] J.Zhu, Y. Shi, X. Zhang, H. Yan, and K. Yan, “Current Density and Efficiency of a Novel Lab ESP for Fine Particles Collection," In Electrostatic Precipitation. 11th International Conference on Electrostatic Precipitation, Hangzhou, 2008, Springer Science & Business Media, p. 65, 2010.

[10] H. Wenge, and X. Haowang, “Non-static Collection Process of the electrostatic Precipitator, “ In Electrostatic Precipitation, Springer, Berlin, Heidelberg, pp. 79-83, 2009.

[11] k. Huang, “Sparck and its effect on electrostatic precipitation,” Paper 5B1, ICESP X, Australia, 2006.

[12] X. Xiaodong, W. Ying, and C. Wangsheng, “Experimental investigation on the collection of fine dust with high resistivity by a bipolar discharging ESP,“In Electrostatic Precipitation, Springer, Berlin, Heidelberg, pp. 87-90, 2009.

[13] A. Jaworek, T. Czech, E. Rajch, and M. Lackowski, “Laboratory studies of back-discharge in fly ash, “Journal of electrostatics, vol. 64, no. 5, pp. 326-337, 2006.

[14] R. E. Bickelhaupt, “A technique for predicting fly ash resistivity. Final report, “no. PB-80-102379, Southern Research Inst., Birmingham, AL (USA), 1979.

[15] Instruction Manual SL Series High Voltage Power Supply.Spellman high voltage Electronics Corporation [Online].Available: http://www.spellmanhv.com.

[16] H. Wiggers and S. Nasri, “Dust resistivity measurements by typical current densuties in electrostatic precipitators, “(in German: Staubwiderstands-messungenbeiElektrofiltertypischen189 Majidandal.Stromdichten), Gefahrstoffe- Reinhaltung der Luft., vol. 68, pp. 177-181, 2008.